International Multilingual Journal of Science and Technology (IMJST)
ISSN: 2528-9810
Vol. 7 Issue 5, May - 2022

Visibility Time Computation For Highly Eccentric Tundra Orbit Satellites

Akpasam Joseph Ekanem[1]
Department of Electrical and Electronic Engineering,
Akwa Ibom State University
Mkpat Enin, Akwa Ibom State

Ezeh, H. I[2]
Dept. Of Cyber Security,
Federal University of Technology, Owerri

Namnsowo Edet Akpan[3]
Department of Electrical/Electronic Engineering Technology
Akwa Ibom State Polytechnic, Ikot Osurua , Akwa Ibom State
namnsowoakpan@gmail.com

***Abstract*— In this paper, the computation of the visibility time for highly eccentric tundra orbit satellites with restriction on the minimum elevation angle is presented. The Study considered four satellites in the tundra orbit category, namely; COSMOS 2546, COSMOS 2541, COSMOS 2518 and COSMOS 2510. The orbital altitude and eccentricity for each of the four satellites were used to determine the orbital period and hence the orbital visibility time for different minimum elevation angle ranging from 0° to 12°. The results showed that the visibility time increases with increase in eccentricity of the orbit. Hence, with 0° minimum elevation angle, COSMOS 2546 satellite with the least eccentricity of 0.668 has the lowest visibility time of 10.666 hours per orbital period of 11.970 hours which gives 89.108 % of visibility time with respect to its orbital period. On the other hand, COSMOS 2518 satellite with the highest eccentricity of 0.704 has the highest visibility time of 10.864 hours per orbital period of 11.968 hours which gives 90.864 % of visibility time with respect to its orbital period. Again, the results of the visibility time of the four tundra orbit satellites (COSMOS 2546, COSMOS 2541, COSMOS 2518 and COSMOS 2510) considered in the study for the case of minimum elevation angle ranging from 0° to 12° show that the visibility time decreases with increase in the minimum elevation angle restriction. For instance, for the COSMOS 2546 satellite, the visibility time decreased from 10.666 hours at minimum elevation angle restriction of 0° to visibility time of 9.244 hours at minimum elevation angle restriction of 12°. In all, the Results showed that the visibility time increases with increase in eccentricity but the visibility time decreases with increase in the minimal elevation angle restriction.**

Keywords*— *Visibility Tim, Highly Eccentric orbit, Satellites, Tundra Orbit Eccentricity. Orbital Period

1. Introduction

Today, satellites are deployed for diverse applications, among them are weather forecasting, radio and TV broadcast, military operations, navigation, global telephone backbones, global mobile communication and other emerging forms of applications [1,2,3,4,5,6,7,8,9,10]. The satellites are launched into orbit and they communicate with earth stations and other satellites from their orbits. The specific nature of satellite and the specific nature of their orbits depends among other things on their specific application and the region of the earth they are meant to cover [11,12, 13,14, 15,16, 17,18]. For instance, geo-stationary orbit satellite orbits the earth at an altitude of about 35,800 kilometers and are located directly above the equator thereby covering the regions around the equator [19,20,21,22,23]. Such satellite does not cover the polar and the high-latitude regions [24, 25,26,27,28,29,30]. In such case, the satellite is never visible to people or earth stations in such region. As such, different orbit is required for effective coverage of the polar and the high-latitude regions [31,32,33,34,35,36,37,38,39,40,41].

One of such orbits targeted at coverage of the polar and the high-latitude regions is the Tundra orbit. Tundra orbit is a form of orbit that is geosynchronous and at the same time highly elliptical; it also has high inclination (of about 63.4°) [41,42,43,44,45,46,47]. The satellites operating in Tundra orbits have apogee dwell that makes them suitable for communication in the high-latitude regions [48,49, 50,51, 52,53,54,55,56]. The Tundra orbit was originally used by Russia for missile early warning satellites [57,58,58,60]. In this paper, the focus is on the determination of the visibility time of the tundra orbit satellite to the earth stations. The visibility time defines the amount of time in each orbital period to which an earth station can see and hence communicate with the satellite in orbit [61,62,63,64,65,65]. In view of the fact that Tundra orbits are highly eccentric, the visibility computation is highly dependent on the orbital eccentricity. The mathematical expressions are presented and four Tundra orbit satellites, namely; COSMOS 2546, COSMOS 2541, COSMOS 2518 and COSMOS 2510 [67,68] are used for numerical examples.

2. Methodology

Tundra orbit is a type of highly eccentric elliptical orbit. The diagram for modelling the satellite visibility time of a Tundra orbit with restriction on the minimal elevation angle above the horizon is shown in Figure 1 **[69].** In this case of satellite with highly eccentric elliptical orbit, the visibility time (Δt_{VH}) can be determined from the knowledge of the eccentricity, e of the orbit and the orbital period, T_o. First, the mean anomaly denoted as $M(B_1)$ is estimated from the eccentricity as follows [69];

$$M(e) = 2\left(\tan^{-1}\left(\sqrt{\frac{(1-e)}{(1+e)}}\right)\right) - \left(e\left(\sqrt{(1-e^2)}\right)\right) \quad \textbf{(1)}$$

Then, the visibility time (Δt_{VH}) is given as [69];

$$\Delta t_{VH} = \left(1 - \frac{M(e)}{\pi}\right) T_o \quad \textbf{(2)}$$

If a limit of ε_{min} is placed on the minimum elevation angle, then, the visibility time window for the satellite is reduced by a factor given as,[70];

$$\Delta t_{VHR} \leq \Delta t_{VH}\left(1 - \frac{2}{\pi}(\varepsilon_{min})\right) \quad (3)$$

The value of Δt_{VHR} is in seconds and it can be expressed in minutes ($\Delta t_{VHR(\min)}$), as well as in hours ($\Delta t_{VHR(\mathrm{hr})}$), as follows;

$$\Delta t_{VHR(\min)} \frac{\Delta t_{VHR}}{60} \quad (4)$$

$$\Delta t_{VHR(\mathrm{hr})} \frac{\Delta t_{VHR}}{3600} \quad (5)$$

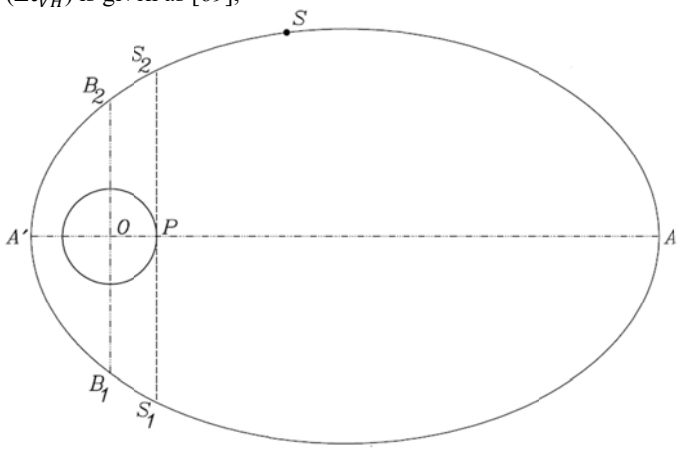

Figure 1 The diagram for satellite visibility time of a highly eccentric elliptical orbit with restriction on the minimal elevation angle above the horizon **[69]**

3. The Case Study Satellite

Tundra orbit is a form of orbit that is geosynchronous and at the same time highly elliptical; it also has high inclination (of about 63.4°). The satellites with Tundra orbit are considered in this study. The four satellites in that category are COSMOS 2546, COSMOS 2541, COSMOS 2518 and COSMOS 2510, and some of the orbital parameters are presented in Table 1. The simulated orbit tracks of the four Tundra orbit satellites (COSMOS 2546, COSMOS 2541, COSMOS 2518 and COSMOS 2510) considered in the study as presented by Satellite Catalog (SATCAT) [69] are shown in Figure 2.

The ground footprint and orbit track for the Tundra orbit satellite (COSMOS 2510) as presented by www.n2yo.com online satellite tool I presented in Figure 3 while the history of some orbital elements for the Tundra orbit satellite (COSMOS 2510) as presented by in-the-sky.org for the period from 19th of February 2022 to 18th of March 2022 is presented in Table 2 . The graph of mean orbital altitude versus time for Tundra orbit satellite (COSMOS 2510) as presented by in-the-sky.org is presented in Figure 4. Also, the graph of orbital inclination versus time for Tundra orbit satellite (COSMOS 2510) as presented by in-the-sky.org is presented in Figure 5. In addition, the graph of orbital eccentricity versus time for Tundra orbit satellite (COSMOS 2510) as presented by in-the-sky.org is presented in Figure 6.

Table 1 The requisite orbital details for the four Tundra orbit satellites (COSMOS 2546, COSMOS 2541, COSMOS 2518 and COSMOS 2510) considered in the study

Parameter	COSMOS 2546	COSMOS 2541	COSMOS 2518	COSMOS 2510
Inclination	63.327°	63.337°	63.074°	62.828°
Eccentricity	0.66799	0.70126	0.70399	0.67486
RA ascending node	15.361 hr	21.169 hr	6.651 hr	11.923 hr
Argument perihelion	268.174°	270.245°	265.687°	270.805°
Mean anomaly	154.878°	311.791°	147.149°	18.735°
Orbital period	717.892 min	717.944 min	717.804 min	717.123 min
Semi major axis	26558 km	26560 km	26556 km	26539 km
Min Altitude	2446.5 km	1563.4 km	1489.8 km	2257.9 km
Mean Altitude	20187.3 km	20188.5 km	20185.1 km	20168.3 km
Peak Altitude	37928.0 km	38813.7 km	38880.4 km	38078.7 km

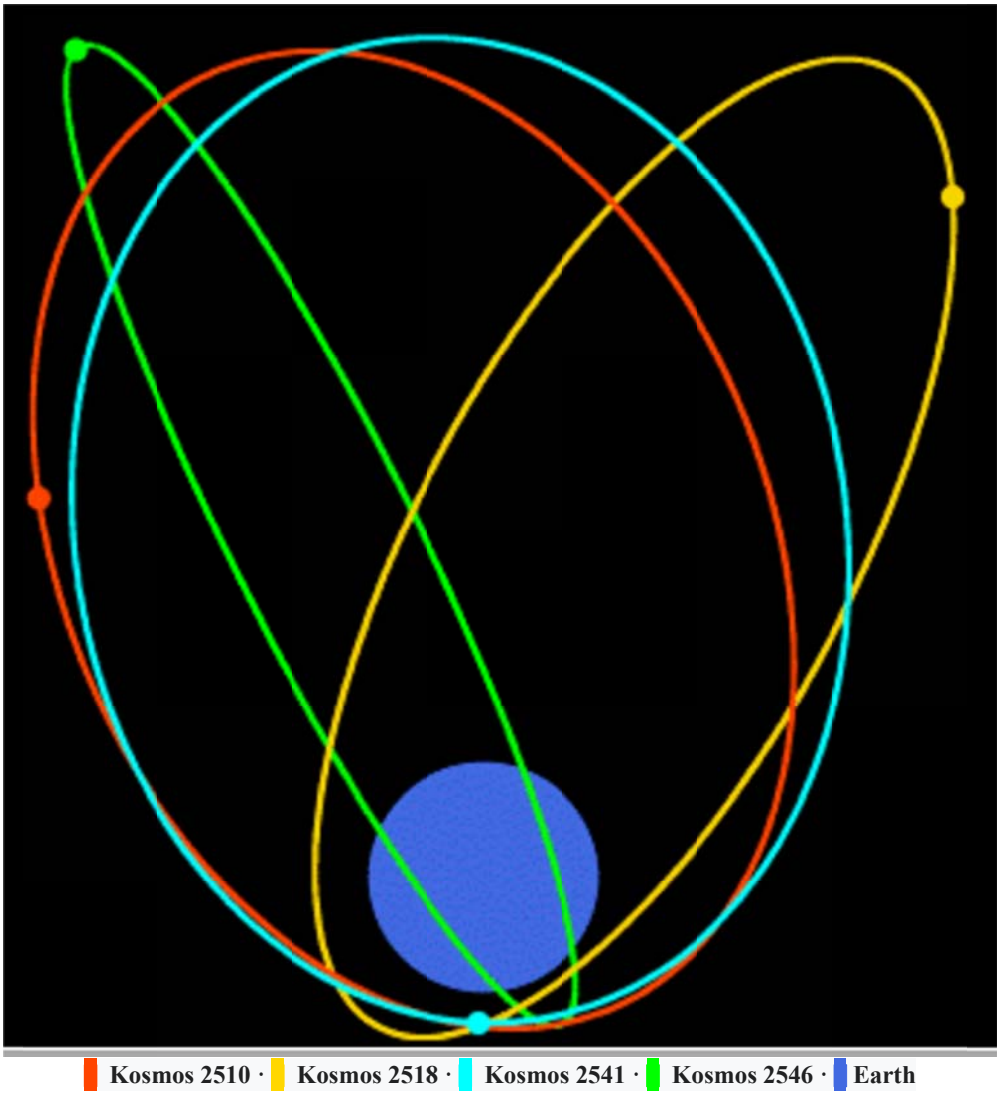

Figure 2 The simulated orbit tracks of the four Tundra orbit satellites (COSMOS 2546, COSMOS 2541, COSMOS 2518 and COSMOS 2510) considered in the study as presented by Satellite Catalog (SATCAT) Data source [69]

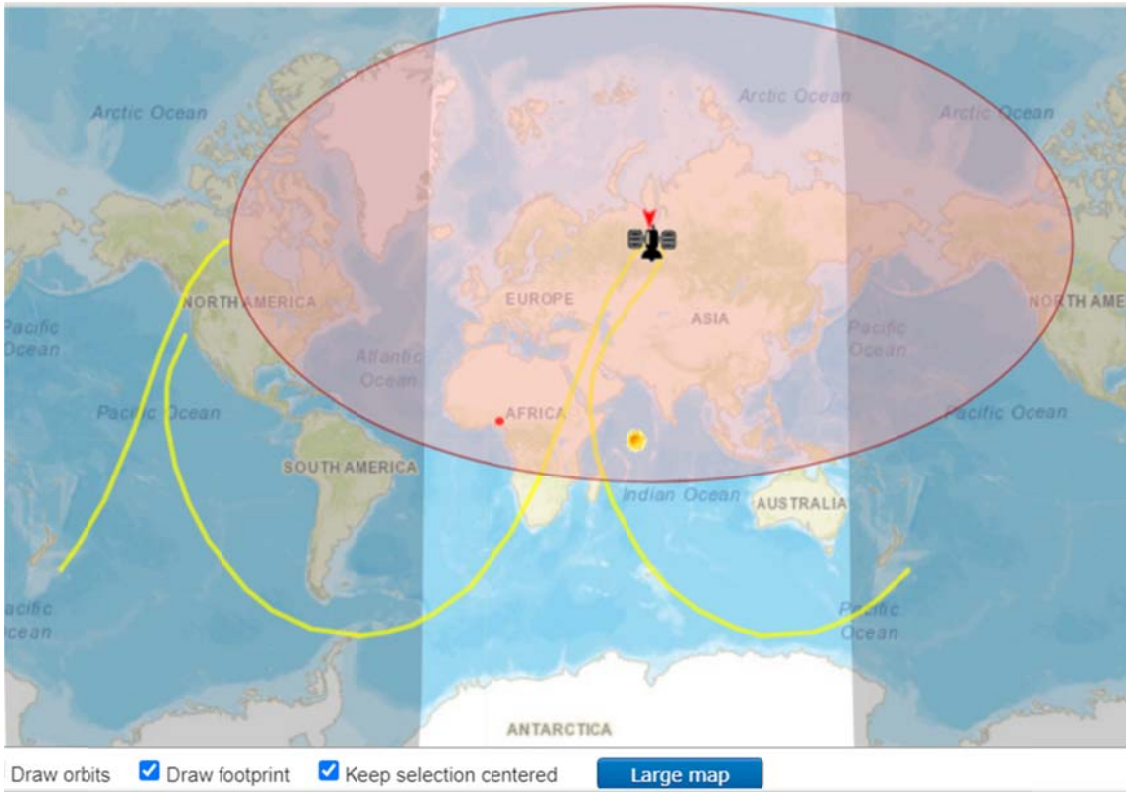

Figure 3 The ground footprint and orbit track for the Tundra orbit satellite (COSMOS 2510) as presented by www.n2yo.com online satellite tool. Source [71]

Table 2 History of some orbital elements for the Tundra orbit satellite (COSMOS 2510) as presented in-the-sky.org for the period from 19th of February 2022 to 18th of March 2022.

Date fetched	Epoch osculation	Inc. [°]	Ecc.	RA asc node [hr]	Arg Peri. [°]	Mean anom [°]	Mean motion [rev/day]
2022 Mar 18 18:54	2022 Mar 16 23:12:04	62.8279	0.67486	11.9226	270.8045	18.7351	2.00802
2022 Mar 17 18:54	2022 Mar 07 12:06:13	62.8228	0.67481	11.9886	270.8195	18.7351	2.00802
2022 Mar 16 18:54	2022 Mar 07 12:06:13	62.8228	0.67481	11.9886	270.8195	18.7351	2.00802
2022 Mar 15 18:54	2022 Mar 07 12:06:13	62.8228	0.67481	11.9886	270.8195	18.7351	2.00802
2022 Mar 14 18:54	2022 Mar 07 12:06:13	62.8228	0.67481	11.9886	270.8195	18.7351	2.00802
2022 Mar 13 18:54	2022 Mar 07 12:06:13	62.8228	0.67481	11.9886	270.8195	18.7351	2.00802
2022 Mar 12 18:53	2022 Mar 07 12:06:13	62.8228	0.67481	11.9886	270.8195	18.7351	2.00802
2022 Mar 11 18:54	2022 Mar 07 12:06:13	62.8228	0.67481	11.9886	270.8195	18.7351	2.00802
2022 Mar 10 18:54	2022 Mar 04 05:57:55	62.8064	0.67491	12.0099	270.8231	18.7351	2.00802
2022 Mar 09 18:54	2022 Mar 04 05:57:55	62.8064	0.67491	12.0099	270.8231	18.7351	2.00802
2022 Mar 08 18:54	2022 Mar 04 05:57:55	62.8064	0.67491	12.0099	270.8231	18.7351	2.00802
2022 Mar 07 18:54	2022 Mar 04 05:57:55	62.8064	0.67491	12.0099	270.8231	18.7351	2.00802
2022 Mar 06 18:54	2022 Mar 04 05:57:55	62.8064	0.67491	12.0099	270.8231	18.7351	2.00802
2022 Mar 05 18:54	2022 Mar 04 05:57:55	62.8064	0.67491	12.0099	270.8231	18.7351	2.00802
2022 Mar 04 18:54	2022 Feb 24 13:07:07	62.8173	0.67474	12.0649	270.8368	18.7351	2.00802
2022 Mar 03 18:54	2022 Feb 24 13:07:07	62.8173	0.67474	12.0649	270.8368	18.7351	2.00802
2022 Mar 02 18:54	2022 Feb 24 13:07:07	62.8173	0.67474	12.0649	270.8368	18.7351	2.00802
2022 Mar 01 18:54	2022 Feb 24 13:07:07	62.8173	0.67474	12.0649	270.8368	18.7351	2.00802
2022 Feb 28 18:54	2022 Feb 24 13:07:07	62.8173	0.67474	12.0649	270.8368	18.7351	2.00802
2022 Feb 27 18:56	2022 Feb 24 13:07:07	62.8173	0.67474	12.0649	270.8368	18.7351	2.00802
2022 Feb 26 18:54	2022 Feb 17 01:47:33	62.8150	0.67470	12.1169	270.8484	18.7351	2.00802
2022 Feb 25 18:54	2022 Feb 17 01:47:33	62.8150	0.67470	12.1169	270.8484	18.7351	2.00802

Date fetched	Epoch osculation	Inc. [°]	Ecc.	RA asc node [hr]	Arg Peri. [°]	Mean anom [°]	Mean motion [rev/day]
2022 Feb 24 18:55	2022 Feb 17 01:47:33	62.8150	0.67470	12.1169	270.8484	18.7351	2.00802
2022 Feb 23 18:54	2022 Feb 17 01:47:33	62.8150	0.67470	12.1169	270.8484	18.7351	2.00802
2022 Feb 22 18:54	2022 Feb 17 01:47:33	62.8150	0.67470	12.1169	270.8484	18.7351	2.00802
2022 Feb 21 18:54	2022 Feb 17 01:47:33	62.8150	0.67470	12.1169	270.8484	18.7351	2.00802
2022 Feb 20 18:54	2022 Feb 17 01:47:33	62.8150	0.67470	12.1169	270.8484	18.7351	2.00802
2022 Feb 19 18:54	2022 Feb 12 14:11:23	62.8127	0.67470	12.1482	270.8539	18.7351	2.00802

(Source: https://in-the-sky.org/spacecraft_elements.php?id=41032)

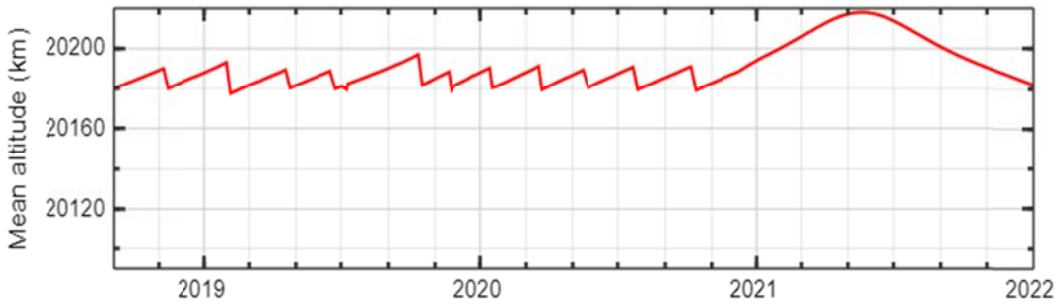

Figure 4 The graph of mean orbital altitude versus time for Tundra orbit satellite (COSMOS 2510) as presented by in-the-sky.org

Figure 5 The graph of mean inclination versus time for Tundra orbit satellite (COSMOS 2510) as presented by in-the-sky.org

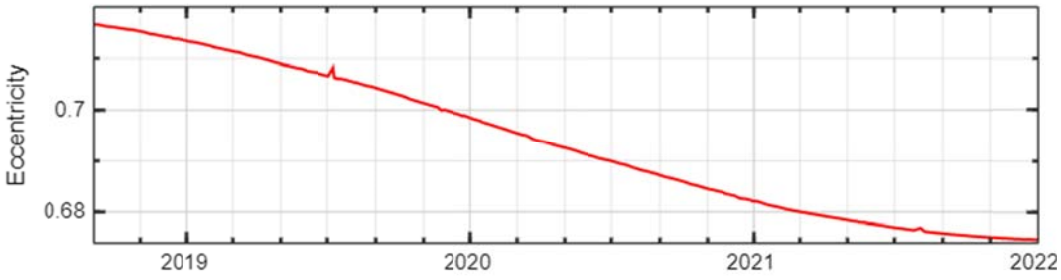

Figure 6 The graph of orbital eccentricity versus time for Tundra orbit satellite (COSMOS 2510) as presented by in-the-sky.org

3. Results and Discussion

The results of the visibility time of the four Tundra orbit satellites (COSMOS 2546, COSMOS 2541, COSMOS 2518 and COSMOS 2510) considered in the study for the case of 0° minimum elevation angle are in Table 3 and Figure 7, Figure 8 and Figure 9. The results showed that the visibility time increases with increase in eccentricity of the orbit. Hence, COSMOS 2546 satellite with the least eccentricity of 0.668 has the lowest visibility time of 10.666 hours per orbital period of 11.970 hours which gives 89.108 % of visibility time with respect to its orbital period. On the other hand, COSMOS 2518 satellite with the highest eccentricity of 0.704 has the highest visibility time of 10.864 hours per orbital period of 11.968 hours which gives 90.864 % of visibility time with respect to its orbital period.

Table 3 The results of the visibility time of the four Tundra orbit satellites (COSMOS 2546, COSMOS 2541, COSMOS 2518 and COSMOS 2510) considered in the study for the case of 0° minimum elevation angle

COSMOS satellite Orbital Altitude, h (km)	COSMOS Satellite Eccentricity, e	COSMOS satellite Orbital Period, To (hour)	COSMOS satellite visibility time in hour	Percentage of visibility time per period (%)
20,187.300	0.668	11.970	10.666	89.108
20,168.300	0.675	11.957	10.693	89.432
20,188.500	0.701	11.971	10.851	90.651
20,185.100	0.704	11.968	10.864	90.775

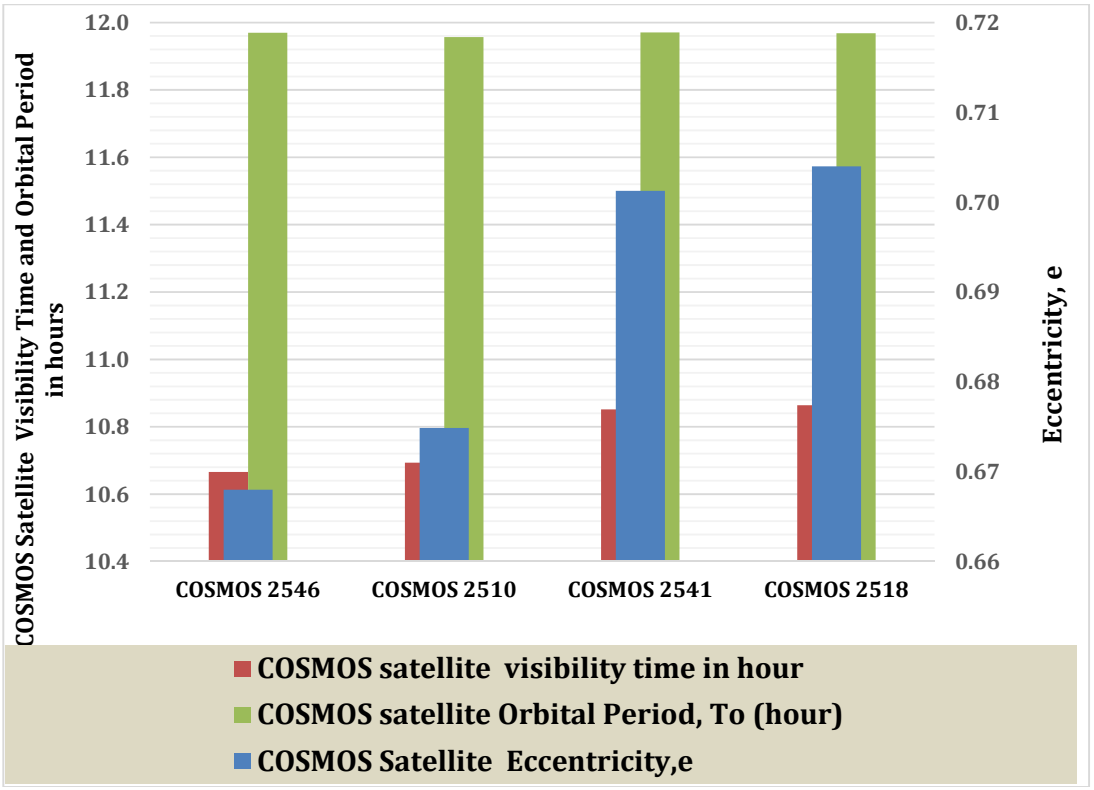

Figure 7 The bar chart of the results of the visibility time, orbital period, and eccentricity of the four Tundra orbit satellites (COSMOS 2546, COSMOS 2541, COSMOS 2518 and COSMOS 2510) considered in the study for the case of 0° minimum elevation angle

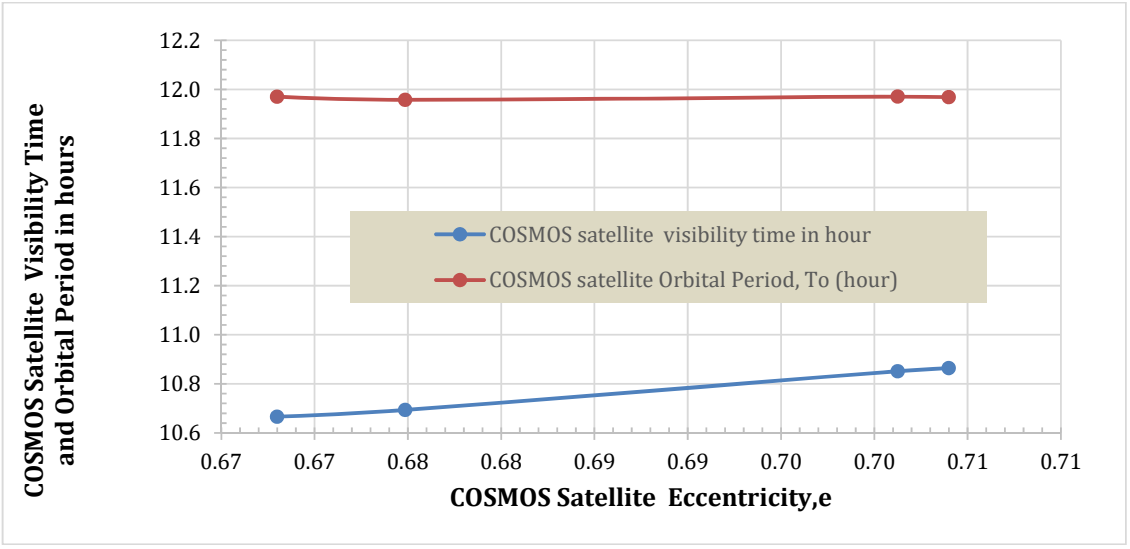

Figure 8 The graph of the visibility time and orbital period verses eccentricity for the four Tundra orbit satellites (COSMOS 2546, COSMOS 2541, COSMOS 2518 and COSMOS 2510) considered in the study for the case of 0° minimum elevation angle

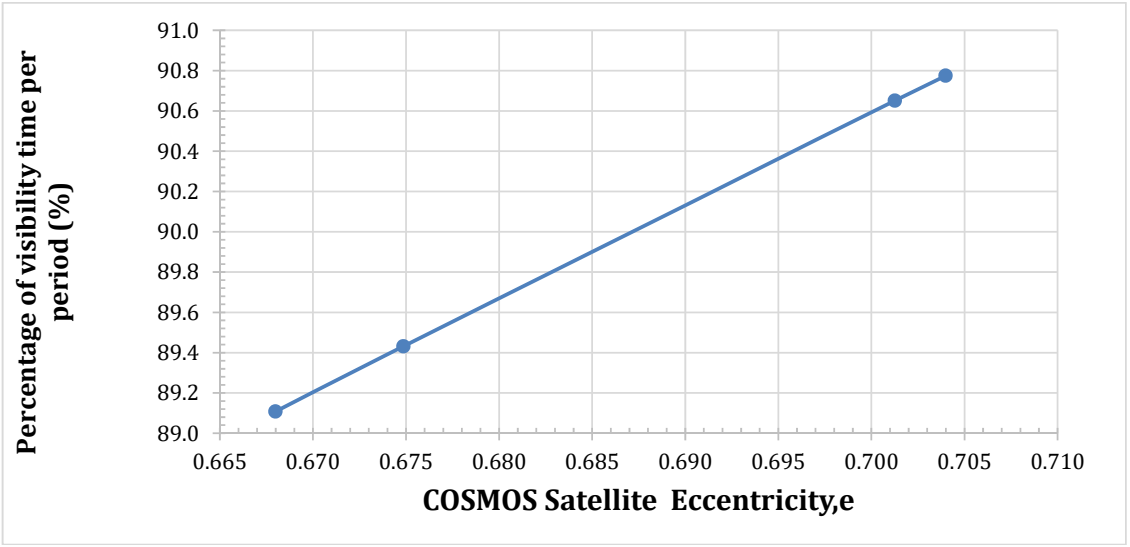

Figure 9 The graph of the percentage of visibility time per orbital period verses eccentricity for the four Tundra orbit satellites (COSMOS 2546, COSMOS 2541, COSMOS 2518 and COSMOS 2510) considered in the study for the case of 0° minimum elevation angle

Again, the results of the visibility time of the four Tundra orbit satellites (COSMOS 2546, COSMOS 2541, COSMOS 2518 and COSMOS 2510) considered in the study for the case of minimum elevation angle ranging from 0° to 12° are in Table 4 and Figure 10. The results show that the visibility time decreases with increase in the minimum elevation angle restriction. For instance, for the COSMOS 2546 satellite, the visibility time decreased from 10.666 hours at minimum elevation angle restriction of 0° to visibility time of 9.244 hours at minimum elevation angle restriction of 12°.

Also, the results of the percentage of visibility time per orbital period of the four Tundra orbit satellites (COSMOS 2546, COSMOS 2541, COSMOS 2518 and COSMOS 2510) considered in the study for the case of minimum elevation angle ranging from 0° to 12° are in Table 5, Figure 11 and Figure 12. The results show that the percentage of visibility time per orbital period decreases with increase in the minimum elevation angle restriction. For instance, for the COSMOS 2546 satellite, the percentage of visibility time per orbital period decreased from 89.108 % at minimum elevation angle restriction of 0° to a value of 77.227 % at minimum elevation angle restriction of 12°.

Table 4 The results of the visibility time of the four Tundra orbit satellites (COSMOS 2546, COSMOS 2541, COSMOS 2518 and COSMOS 2510) considered in the study for the case of minimum elevation angle ranging from 0° to 12°

Satellite Name	COSMOS Satellite Eccentricity, e	COSMOS satellite visibility time in hour, Emin =0°	COSMOS satellite visibility time in hour, Emin =4°	COSMOS satellite visibility time in hour, Emin =8°	COSMOS satellite visibility time in hour, Emin =12°
COSMOS 2546	0.66799	10.666	10.192	9.718	9.244
COSMOS 2510	0.67486	10.693	10.218	9.743	9.267
COSMOS 2541	0.70126	10.851	10.369	9.887	9.405
COSMOS 2518	0.70399	10.864	10.381	9.898	9.416

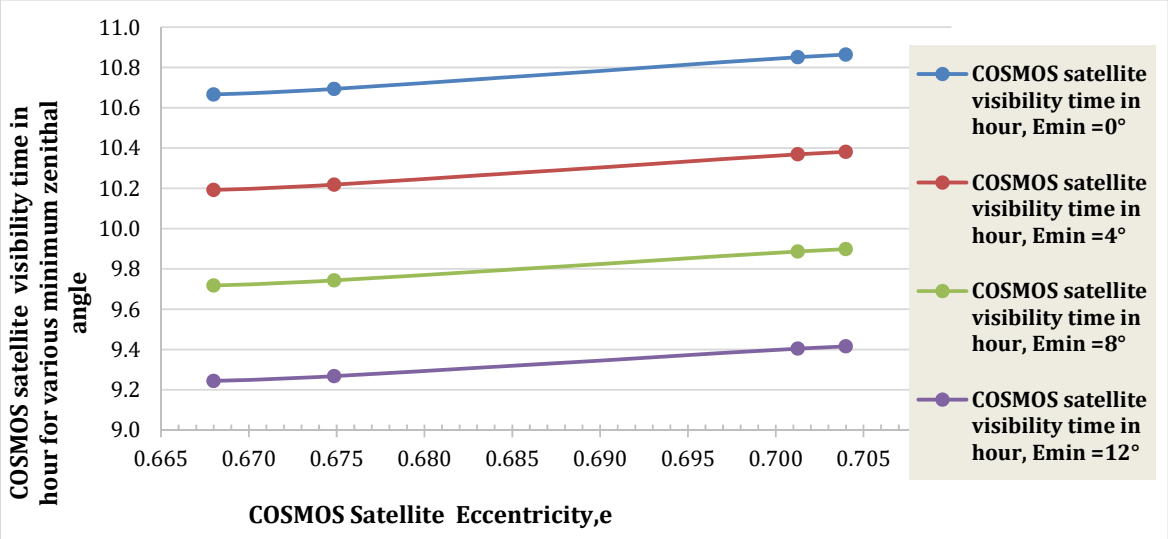

Figure 10 The graph of the percentage of visibility time per orbital period verses eccentricity for the four Tundra orbit satellites (COSMOS 2546, COSMOS 2541, COSMOS 2518 and COSMOS 2510) considered in the study for the case of minimum elevation angle ranging from 0° to 12°

Table 5 The results of the percentage of visibility time per orbital period of the four Tundra orbit satellites (COSMOS 2546, COSMOS 2541, COSMOS 2518 and COSMOS 2510) considered in the study for the case of minimum elevation angle ranging from 0° to 12°

Satellite Name	COSMOS Satellite Eccentricity, e	Percentage of visibility time per orbital period (%), Emin =0°	Percentage of visibility time per orbital period (%), Emin =4°	Percentage of visibility time per orbital period (%), Emin =8°	Percentage of visibility time per orbital period (%), Emin =12°
COSMOS 2546	0.66799	89.108	85.147	81.187	77.227
COSMOS 2510	0.67486	89.432	85.457	81.482	77.508
COSMOS 2541	0.70126	90.651	86.622	82.593	78.564
COSMOS 2518	0.70399	90.775	86.740	82.706	78.672

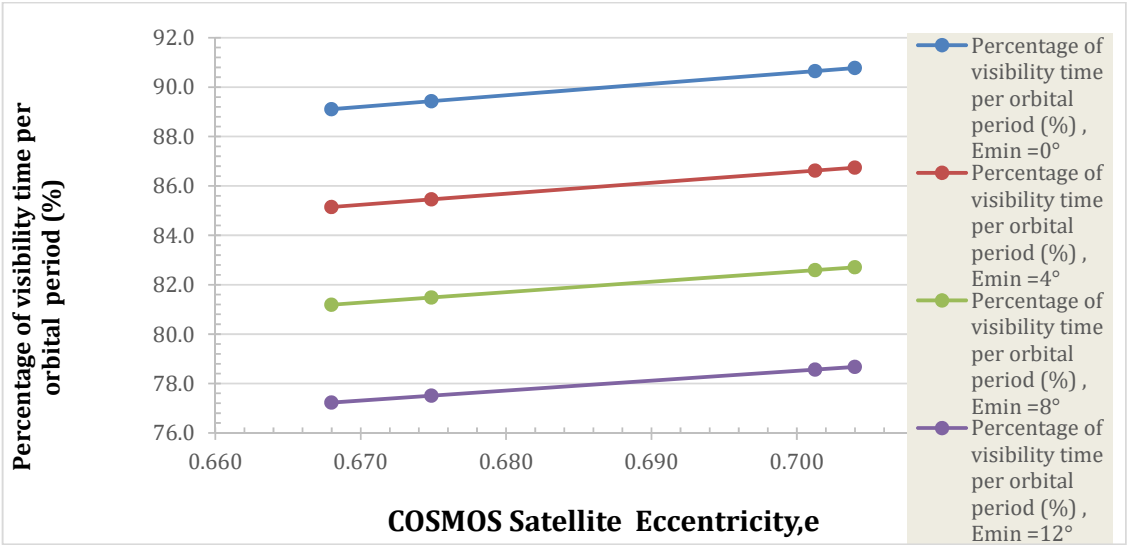

Figure 11 The graph of the percentage of visibility time per orbital period verses eccentricity for the four Tundra orbit satellites (COSMOS 2546, COSMOS 2541, COSMOS 2518 and COSMOS 2510) considered in the study for the case of minimum elevation angle ranging from 0° to 12°

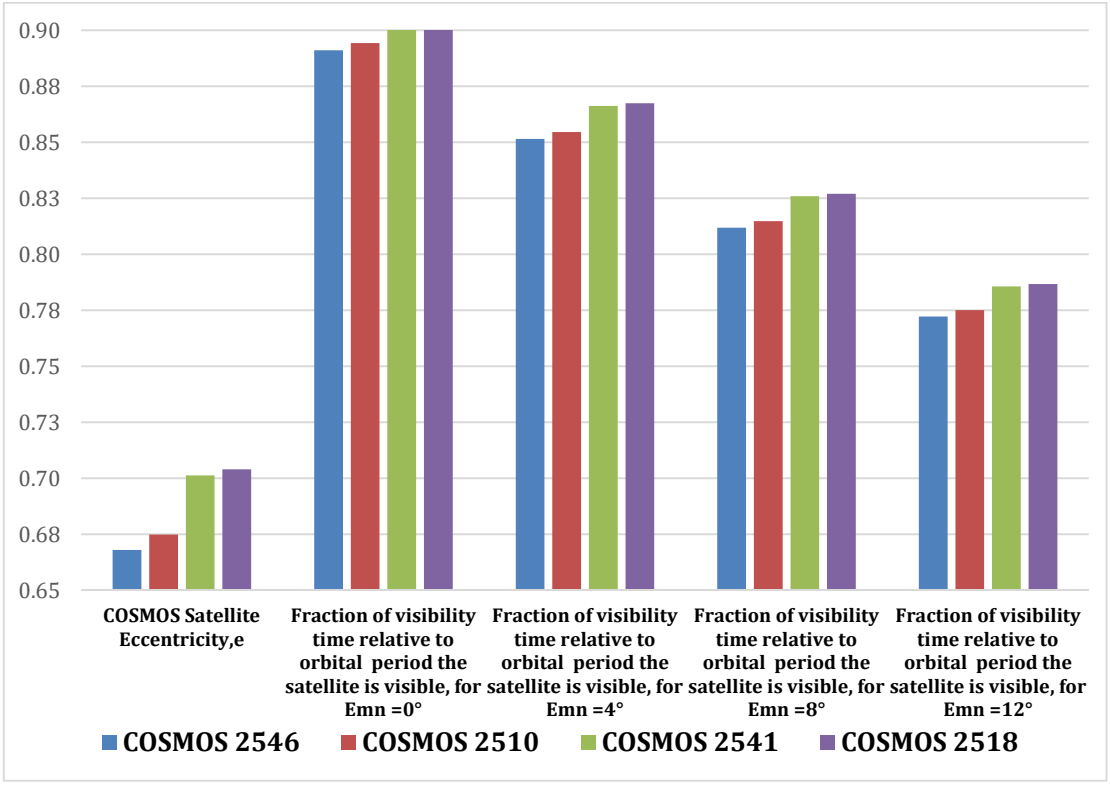

Figure 12 The bar chart of the eccentricity and fraction of visibility time relative to orbital period for the four Tundra orbit satellites (COSMOS 2546, COSMOS 2541, COSMOS 2518 and COSMOS 2510) considered in the study for the case of 0° minimum elevation angle

4. Conclusion

The commutation visibility time of four highly eccentric tundra orbit satellites is presented. The computation examined the impact of the minimal elevation angle on the visibility time. Also, the variation of the satellite visibility time with the eccentricity of the orbit is considered. The Results showed that the visibility time increases with increase in eccentricity but the visibility time decreases with increase in the minimal elevation angle restriction.

References

1. Kumar, S., & Moore, K. B. (2002). The evolution of global positioning system (GPS) technology. *Journal of science Education and Technology*, *11*(1), 59-80.

2. Ilcev, S. D. (2005). *Global Mobile Satellite Communications: For Maritime, Land and Aeronautical Applications*. Springer Science & Business Media.

3. **Simeon, Ozuomba. (2017).** "Determination Of The Clear Sky Composite Carrier To Noise Ratio For Ku-Band Digital Video Satellite Link" ***Science and Technology Publishing*** *(SCI & TECH) Vol. 1 Issue 7, July – 2017*

4. Kumar, S. (2015). *Wireless Communications Fundamental & Advanced Concepts: Design Planning and Applications* (Vol. 41). River Publishers.

5. Rawat, P., Singh, K. D., Chaouchi, H., & Bonnin, J. M. (2014). Wireless sensor networks: a survey on recent developments and potential synergies. *The Journal of supercomputing*, *68*(1), 1-48.

6. **Simeon, Ozuomba. (2016)** "Comparative Analysis Of Rain Attenuation In Satellite Communication Link For Different Polarization Options." ***Journal of Multidisciplinary Engineering Science and Technology*** *(JMEST) Vol. 3 Issue 6, June - 2016*

7. Pal, S., & Rao, V. S. (2007). Satellite technology utilization for rural and urban India. *IETE Technical Review*, *24*(4), 277-286.

8. **Simeon, Ozuomba Ozuomba (2014)** "Comparative Evaluation Of Initial Value Options For Numerical Iterative Solution To Eccentric Anomalies In Kepler's Equation For Orbital Motion." ***Journal of Multidisciplinary Engineering Science and Technology (JMEST)*** *Vol. 1 Issue 5, December - 2014*

9. Murtaza, A., & Jianwei, L. (2019, April). Multipurpose IP-based space air-ground information network. In *Journal of Physics: Conference Series* (Vol. 1187, No. 4, p. 042044). IOP Publishing.

10. **Simeon, Ozuomba (2014)** "Fixed Point Iteration Computation Of Nominal Mean Motion And Semi Major Axis Of Artificial Satellite Orbiting An Oblate Earth." ***Journal of Multidisciplinary Engineering Science and Technology (JMEST)*** *Vol. 1 Issue 4, November – 2014*

11. Dawson, L. (2018). Satellite Technology. In *War in Space* (pp. 131-156). Springer, Cham.

12. Agama, F. O. (2017). Effects of the Bogota Declaration on the legal status of geostationary orbit in international space law. *Nnamdi Azikiwe University Journal of International Law and Jurisprudence*, *8*(1), 24-34.

13. Rosengren, A. J., Skoulidou, D. K., Tsiganis, K., & Voyatzis, G. (2019). Dynamical cartography of Earth satellite orbits. *Advances in Space Research*, *63*(1), 443-460.

14. Ferrer, T., Céspedes, S., & Becerra, A. (2019). Review and evaluation of MAC protocols for satellite IoT systems using nanosatellites. *Sensors*, *19*(8), 1947.

15. Belward, A. S., & Skøien, J. O. (2015). Who launched what, when and why; trends in global land-cover observation capacity from civilian earth observation satellites. *ISPRS Journal of Photogrammetry and Remote Sensing*, *103*, 115-128.

16. Boley, A. C., & Byers, M. (2021). Satellite mega-constellations create risks in Low Earth Orbit, the atmosphere and on Earth. *Scientific Reports*, *11*(1), 1-8.

17. El-Ghany, A., Nesreen, M., El-Aziz, A., Shadia, E., & Marei, S. S. (2020). A review: Application of remote sensing as a promising strategy for insect pests and diseases management. *Environmental Science and Pollution Research*, *27*(27), 33503-33515.

18. **Simeon, Ozuomba. (2015)** "Development of Closed-Form Approximation of the Eccentric Anomaly for Circular and Elliptical Keplerian Orbit." Development 2.6 (2015). ***Journal of Multidisciplinary Engineering Science and Technology*** *(JMEST) Vol. 2 Issue 6, June - 2015*

19. Singh, K., Nirmal, A. V., & Sharma, S. V. (2017). Link margin for wireless radio communication link. *ICTACT Journal on Communication Technology*, *8*(3), 1574-1581.

20. Khan, M. R. H., Ziad, M. O., Chowa, S. M., & Mehedi, M. (2021). *A comparative study of intelligent reflecting surface and relay in satellite communication* (Doctoral dissertation, Brac University).

21. **Simeon, Ozuomba. (2016)** "Development And Application Of Complementary Root-Based Seeded Secant Iteration For Determination Of Semi Major Axis Of Perturbed Orbit" *International Multilingual Journal of Science and Technology (IMJST) Vol. 1 Issue 2, July – 2016*

22. Loge, L. (2014). Radiation Environment Analysis of Highly Elliptical Orbits for Satellite Based Broadband Communications to the Arctic. In *32nd AIAA International Communications Satellite Systems Conference* (p. 4245).

23. **Simeon, Ozuomba. (2017)** "Development Of Strict Differential Seeded Secant Numerical

Iteration Method For Computing The Semi Major Axis Of A Perturbed Orbit Based On The Anomalistic Period." *Development 1.8 (2017). **Science and Technology Publishing** (SCI & TECH) Vol. 1 Issue 8, August – 2017*

24. De Bruijn, F. J. (2017). *Guidance control and dynamics of a new generation of geostationary satellites* (Doctoral dissertation, Technische Universiteit Delft).
25. Doyle, T., & Seal, G. (Eds.). (2018). *Indian Ocean Futures: New Partnerships, New Alliances, and Academic Diplomacy*. Routledge.
26. Xie, P., & Joyce, R. J. (2014). Integrating information from satellite observations and numerical models for improved global precipitation analyses: Exploring for an optimal strategy. *Remote Sensing of the Terrestrial Water Cycle, Geophys. Monogr*, *206*, 43-60.
27. Maral, G., Bousquet, M., & Sun, Z. (2020). *Satellite communications systems: systems, techniques and technology*. John Wiley & Sons.
28. Qu, Y., Liang, S., Liu, Q., He, T., Liu, S., & Li, X. (2015). Mapping surface broadband albedo from satellite observations: A review of literatures on algorithms and products. *Remote Sensing*, *7*(1), 990-1020.
29. Shou, Y. X., Lu, F., & Shou, S. (2016). A Satellite View of the Atmospheric Dry Intrusion and its Influences on the Mid-Latitude Disastrous Weather.
30. Yang, C. S., Kim, S. H., Ouchi, K., & Back, J. H. (2015). Generation of high resolution sea surface temperature using multi-satellite data for operational oceanography. *Acta Oceanologica Sinica*, *34*(7), 74-88.
31. Xie, Y., Xue, Y., Guang, J., Mei, L., She, L., Li, Y., ... & Fan, C. (2019). Deriving a global and hourly data set of aerosol optical depth over land using data from four geostationary satellites: GOES-16, MSG-1, MSG-4, and Himawari-8. *IEEE Transactions on Geoscience and Remote Sensing*, *58*(3), 1538-1549.
32. Heiligers, J., Parker, J. S., & Macdonald, M. (2018). Novel solar-sail mission concepts for high-latitude Earth and lunar observation. *Journal of Guidance, Control, and Dynamics*, *41*(1), 212-230.
33. Widhalm, B., Bartsch, A., & Goler, R. (2018). Simplified normalization of C-band synthetic aperture radar data for terrestrial applications in high latitude environments. *Remote Sensing*, *10*(4), 551.
34. Cherniak, I., & Zakharenkova, I. (2017). New advantages of the combined GPS and GLONASS observations for high-latitude ionospheric irregularities monitoring: case study of June 2015 geomagnetic storm. *Earth, Planets and Space*, *69*(1), 1-14.
35. Dou, Y., & Liu, X. (2020, July). Design of Global Coverage Satellite Constellation Based on GEO and IGSO. In *International Conference in Communications, Signal Processing, and Systems* (pp. 1276-1282). Springer, Singapore.
36. Chisham, G. (2017). A new methodology for the development of high-latitude ionospheric climatologies and empirical models. *Journal of Geophysical Research: Space Physics*, *122*(1), 932-947.
37. Li, X., Ma, F., Li, X., Lv, H., Bian, L., Jiang, Z., & Zhang, X. (2019). LEO constellation-augmented multi-GNSS for rapid PPP convergence. *Journal of Geodesy*, *93*(5), 749-764.
38. Lee, S., Wu, Y., & Mortari, D. (2016). Satellite constellation design for telecommunication in Antarctica. *International Journal of Satellite Communications and Networking*, *34*(6), 725-737.
39. De Michelis, P., Consolini, G., Tozzi, R., & Marcucci, M. F. (2017). Scaling Features of High-Latitude Geomagnetic Field Fluctuations at Swarm Altitude: Impact of IMF Orientation. *Journal of Geophysical Research: Space Physics*, *122*(10), 10-548.
40. De Michelis, P., Consolini, G., Tozzi, R., & Marcucci, M. F. (2016). Observations of high-latitude geomagnetic field fluctuations during St. Patrick's Day storm: Swarm and SuperDARN measurements. *Earth, Planets and Space*, *68*(1), 1-16.
41. Cherniak, I., & Zakharenkova, I. (2015). Dependence of the high-latitude plasma irregularities on the auroral activity indices: a case study of 17 March 2015 geomagnetic storm. *Earth, Planets and Space*, *67*(1), 1-12.
42. Jenkin, A. B., McVey, J. P., Wilson, J. R., & Sorge, M. E. (2017, April). Tundra disposal orbit study. In *Proceedings of the 7th European Conference on Space Debris, Darmstadt*.
43. Jenkin, A. B., McVey, J. P., Emmert, D. M., & Sorge, M. E. (2021). Comparison of disposal options for Tundra orbits in terms of delta-V cost and long-term collision risk. *Journal of Space Safety Engineering*, *8*(1), 47-62.
44. Li, Z., Schmit, T. J., Li, J., Gunshor, M. M., & Nagle, F. W. (2021). Understanding the imaging capability of Tundra orbits compared to other orbits. *IEEE Transactions on Geoscience and Remote Sensing*, *59*(11), 8944-8956.
45. Zhang, M. J., Zhao, C. Y., Hou, Y. G., Zhu, T. L., Wang, H. B., Sun, R. Y., & Zhang, W. (2017). Long-term dynamical evolution of Tundra-type orbits. *Advances in Space Research*, *59*(2), 682-697.

46. Anderson, R. A. (2014). *Thermal Environment for Polar Communications and Weather System in the Telesat-Tundra Orbit* (Doctoral dissertation, Carleton University).
47. Jenkin, A. B., McVey, J. P., & Sorge, M. E. (2019). Orbital lifetime and collision risk reduction for inclined geosynchronous disposal orbits. *Acta Astronautica*, *161*, 153-165.
48. McGraw, J. T., Zimmer, P. C., & Ackermann, M. R. (2017, September). Ever wonder what's in Molniya? We do. In *Proceedings of the Advanced Maui Optical and Space Surveillance (AMOS) Technologies Conference, Maui, HI, USA* (pp. 19-22).
49. Wang, L., Shahroudi, N., Maddy, E., Garrett, K., Boukabara, S., Hoffman, R., & Ide, K. (2021). Orbit Simulator for Satellite and Near-Space Platforms Supporting Observing System Simulation Experiments. *Journal of Atmospheric and Oceanic Technology*, *38*(12), 2109-2123.
50. Li, Z., Schmit, T. J., Li, J., Gunshor, M. M., & Nagle, F. W. (2021). Understanding the imaging capability of Tundra orbits compared to other orbits. *IEEE Transactions on Geoscience and Remote Sensing*, *59*(11), 8944-8956.
51. Jenkin, A. B., McVey, J. P., Emmert, D. M., & Sorge, M. E. (2021). Comparison of disposal options for Tundra orbits in terms of delta-V cost and long-term collision risk. *Journal of Space Safety Engineering*, *8*(1), 47-62.
52. Fantino, E., Flores Le Roux, R. M., Di Salvo, A., & Di Carlo, M. (2015). Analysis of perturbations and station-keeping requirements in highly-inclined geosynchronous orbits. In *ISSFD 2015: 25th International Symposium on Space Flight Dynamics, 19-23 October, Munich, Germany* (pp. 1-13).
53. Anderson, R. A. (2014). *Thermal Environment for Polar Communications and Weather System in the Telesat-Tundra Orbit* (Doctoral dissertation, Carleton University).
54. Razoumny, Y. N. (2019). Locally Geostationary Orbits: Optimal Geometry of Elliptic Orbit for Earth Coverage. *Journal of Spacecraft and Rockets*, *56*(4), 1017-1023.
55. LeMaster, E. A. (2021, January). A Comparison of Relativistic Impacts on Satellite Timekeeping for Various Orbits. In *Proceedings of the 52nd Annual Precise Time and Time Interval Systems and Applications Meeting* (pp. 326-337).
56. Raghunandan, K. (2022). Satellite Communication. In *Introduction to Wireless Communications and Networks* (pp. 247-275). Springer, Cham.
57. Panda, D. P., Bandi, K., Sastry, P. S. R., & Rambabu, K. (2020). Satellite Constellation Design Studies for Missile Early Warning. In *Advances in Small Satellite Technologies* (pp. 385-396). Springer, Singapore.
58. Acton, J. M. (2018). Escalation through entanglement: How the vulnerability of command-and-control systems raises the risks of an inadvertent nuclear war. *International security*, *43*(1), 56-99.
59. Hsiung, C. W. (2020). Missile defense and early warning missile attack system cooperation: Enhancing the Sino-Russian defense partnership.
60. Barrett, A. M. (2016). False alarms, true dangers. *RAND Corporation document PE-191-TSF, DOI*, *10*.
61. Liu, X., Laporte, G., Chen, Y., & He, R. (2017). An adaptive large neighborhood search metaheuristic for agile satellite scheduling with time-dependent transition time. *Computers & Operations Research*, *86*, 41-53.
62. Jia, X., Lv, T., He, F., & Huang, H. (2017). Collaborative data downloading by using inter-satellite links in LEO satellite networks. *IEEE Transactions on Wireless Communications*, *16*(3), 1523-1532.
63. Wang, X., Han, C., Yang, P., & Sun, X. (2019). Onboard satellite visibility prediction using metamodeling based framework. *Aerospace Science and Technology*, *94*, 105377.
64. Lawler, S. M., Boley, A. C., & Rein, H. (2021). Visibility Predictions for Near-future Satellite Megaconstellations: Latitudes near 50° Will Experience the Worst Light Pollution. *The Astronomical Journal*, *163*(1), 21.
65. Ammar, M. K., Amin, M. R., & Hassan, M. H. M. (2018). Visibility intervals between two artificial satellites under the action of Earth oblateness. *Applied Mathematics and Nonlinear Sciences*, *3*(2), 353-374.
66. Huang, J., Su, Y., Huang, L., Liu, W., & Wang, F. (2016). An optimized snapshot division strategy for satellite network in GNSS. *IEEE Communications Letters*, *20*(12), 2406-2409.
67. https://www.n2yo.com/database/?name=COSMOS#results
68.] Satellite Catalog (SATCAT), accessed at :https://en.wikipedia.org/wiki/File:Animation_of_EKS_orbit_around_Earth.gif
69. Capderou, M. (2002). *Satellites: orbites et missions*. Springer Science & Business Media.
70. Morgan-Jones, I., & Loskot, P. (2019). Regional Coverage Analysis of LEO Satellites with Kepler Orbits. *arXiv preprint arXiv:1910.10704*.
71. https://www.n2yo.com/?s=9880